

# Results of WFC3 Thermal Vacuum Testing: IR Channel Readnoise

---

B. Hilbert  
April 11, 2005

---

## ABSTRACT

*During WFC3's initial thermal vacuum testing campaign in September and October 2004, the readout noise levels for the IR channel were measured. Readnoise values from both full frame and subarray ramps were in agreement with readnoise values previously measured on FPA64 at the Detector Characterization Lab (DCL). Using data from the IR01 and IR05 tests in thermal vacuum testing, WFC3's IR channel readnoise is between  $19.5 e^-/\text{pix}$  and  $22.5 e^-/\text{pix}$  for correlated double sampling (CDS), regardless of array size. The CEI Spec for IR channel CDS readnoise is  $15 e^-/\text{pix}$ .*

---

## Introduction

Prior to thermal vacuum testing at Goddard Space Flight Center in September and October of 2004, the only measurement of readnoise for WFC3's IR channel came from component-level readnoise measurements of FPA64 made at DCL. These measurements were made on 80 ramps with 4-second exposure times, and gave CDS readnoise values of 23.9 - 24.0  $e^-/\text{pix}$  for each quadrant of the detector. (Malumuth, 2004) The goal of the thermal vacuum testing was to obtain readnoise values for the fully integrated IR channel, using sample sequences and subarray sizes available on-orbit.

## Data

Data used for this analysis were taken as part of the IR01 and IR05 tests. The IR01 data included 26 full-frame ramps taken using the RAPID sample sequence. Data from the IR05 test included 6 RAPID ramps and 6 STEP25 ramps of various subarray sizes. A summary of the ramps used for this test is presented in Table 1. All data were taken at the nominal on-orbit gain setting of  $2.5 \text{ e}^-/\text{ADU}$ .

### *List of Observations*

Test	# of Ramps	Array Size (pixels)	Ramp Exposure Time (sec)	Sampl Sequence
IR01	26	1024	67.05	RAPID
IR05	2	512	24.55	RAPID
	2	256	10.16	RAPID
	2	128	4.80	RAPID
IR05	2	512	237.4	STEP25
	2	256	223.0	STEP25
	2	128	217.7	STEP25

**Table 1.** List of data ramps used to calculate readnoise values.

## Analysis

Prior to readnoise analysis, all files were run through the IDL pre-processing pipeline, (Hilbert, 2004) in order to subtract reference pixel values (bias correction), remove bad pixels, and manipulate the data ramps into a more convenient format.

Readnoise values were calculated using two methods. The first method was similar to that used by Eliot (2004) to measure the read noise of FPA64 prior to installation in WFC3. For this calculation, a linear fit was made to the signal up the ramp for each pixel. This fit provided a measure of the dark current up the ramp. Once the dark current rate for the pixel was known, its contribution to the signal was subtracted from the ramp. A histogram was created for each quadrant from the signal in the second read of the ramp. This minimized the effects of any residual dark current and dark current noise, which would increase with read number, as well as any instabilities associated with the first read of the IR detector. A Gaussian was fit to the histogram from each quadrant, the width of which (multiplied by the gain of  $2.5 \text{ e}^-/\text{ADU}$ ) was taken as the readnoise. In order to convert this readnoise into that for correlated double sampling, the Gaussian widths were multiplied by the square root of 15/13 (to account for the line fitting of the 15 reads, and the square

root of 2 (to convert from single read sampling to CDS). The median of the readnoise values for each quadrant is shown in Tables 2 and 3 below.

The second method used to calculate readnoise in the IR channel used difference images (S. Baggett, priv. comm.). Dark current contribution was minimized by taking the differences of consecutive reads within a ramp. For a given pixel, the readnoise was calculated by taking the standard deviation of the values in the difference images at that pixel. This calculation was performed on all pixels, creating a readnoise image. A histogram was created for each quadrant of the readnoise image. Readnoise was then calculated by fitting a Gaussian to the histogram, and multiplying the location of the peak by the gain ( $2.5 \text{ e}^-/\text{ADU}$ ). An example of a typical histogram and gaussian fit is shown in Figure 1. As with the previous method, readnoise values were calculated on each ramp individually and then averaged together to obtain the final readnoise values reported in Tables 2 and 3. While this method does not explicitly remove dark current from the signal, adjacent reads in the RAPID sequence are close enough together in time that dark current is negligible.

Calculated readnoise values for a given quadrant were relatively constant from ramp to ramp with both techniques. Readnoise values for the individual files used to create the medians in Tables 2 and 3 generally varied by no more than  $0.2 \text{ e}^-/\text{pix}$  within a given quadrant. Readnoise values calculated with the line fitting technique were consistently higher than those from the adjacent differences method. The differences can be explained only partially by the dark current noise remaining in the ramp during the line fitting technique. Assuming a dark current rate of  $0.2 \text{ e}^-/\text{pix}/\text{sec}$  (Hilbert, 2005), for the exposure times given in Table 1, dark current noise can increase the total measured noise by up to roughly  $0.12 \text{ e}^-/\text{pix}$ . The observed differences in calculated readnoise levels are most likely due to errors in the line fitting, resulting in incomplete dark current subtraction and residual signal contaminating the readnoise images. Table 4, which gives the subarray readnoise values calculated from longer STEP25 ramps, supports this idea, as the line fitting readnoise values are closer to the adjacent difference readnoise values than when RAPID data are examined, as in Table 3. As a result, the readout noise values obtained with the adjacent differences method are more representative of the true readnoise of FPA64.

	Quadrant A ( $\text{e}^-/\text{pix}$ )	Quadrant B ( $\text{e}^-/\text{pix}$ )	Quadrant C ( $\text{e}^-/\text{pix}$ )	Quadrant D ( $\text{e}^-/\text{pix}$ )
Adjacent Differences	21.97 +/- 0.13	21.43 +/- 0.02	21.27 +/- 0.04	21.69 +/- 0.03
Line Fitting	23.08 +/- 0.14	22.49 +/- 0.07	22.25 +/- 0.08	22.80 +/- 0.06

**Table 2.** Median CDS readnoise values calculated from the full-frame IR01 data, using the two methods described above. The  $1\text{-}\sigma$  uncertainties on the readnoise values in this table are derived from the standard deviation of the readnoise values for the individual frames.

The readnoise calculations described above were also performed on the STEP25 subarray ramps from the IR05 test. Comparing the results in Table 4 with those for the RAPID ramps in Table 3, the effects of the additional dark current associated with the longer exposure times are obvious. The extra dark current provides for a better best-fit line and a more complete removal of signal. The readnoise values from line-fitting the STEP25 ramps are actually lower than those associated with the RAPID ramps. The adjacent difference method however, show very little change in readnoise values between the STEP25 and RAPID data.

## Conclusions

Median IR channel CDS readnoise is roughly constant with subarray size, with values from  $20.2e^-/\text{pix}$  to  $22.5 e^-/\text{pix}$ . These values are consistent with those found at DCL for FPA64 prior to integration into WFC3. These values are roughly 50% higher than the  $15 e^-/\text{pix}$  CDS CEI Spec for IR readnoise. For a typical full frame ramp, 80% (823,000) of the science pixels have readnoise values above spec.

Method	Array Size (pixels)	Quadrant A ( $e^-/\text{pix}$ )	Quadrant B ( $e^-/\text{pix}$ )	Quadrant C ( $e^-/\text{pix}$ )	Quadrant D ( $e^-/\text{pix}$ )
Adjacent Differences	512	21.66 +/- 0.01	21.07 +/- 0.004	20.98 +/- 0.04	21.14 +/- 0.03
Line Fitting		22.99 +/- 0.11	22.10 +/- 0.05	21.99 +/- 0.16	22.22 +/- 0.06
Adjacent Differences	256	21.14 +/- 0.03	20.73 +/- 0.22	20.90 +/- 0.03	20.93 +/- 0.03
Line Fitting		22.60 +/- 0.05	21.91 +/- 0.18	22.05 +/- 0.40	21.91 +/- 0.41
Adjacent Differences	128	20.30 +/- 0.03	20.31 +/- 0.12	21.05 +/- 0.16	20.52 +/- 0.04
Line Fitting		22.74 +/- 0.01	22.06 +/- 0.57	22.12 +/- 0.16	22.28 +/- 0.81

**Table 3.** Median CDS readnoise values calculated from the IR05 RAPID data. Subarray results are based on only 2 ramps per subarray size, resulting in low number statistics when calculating means and uncertainties (standard deviation).

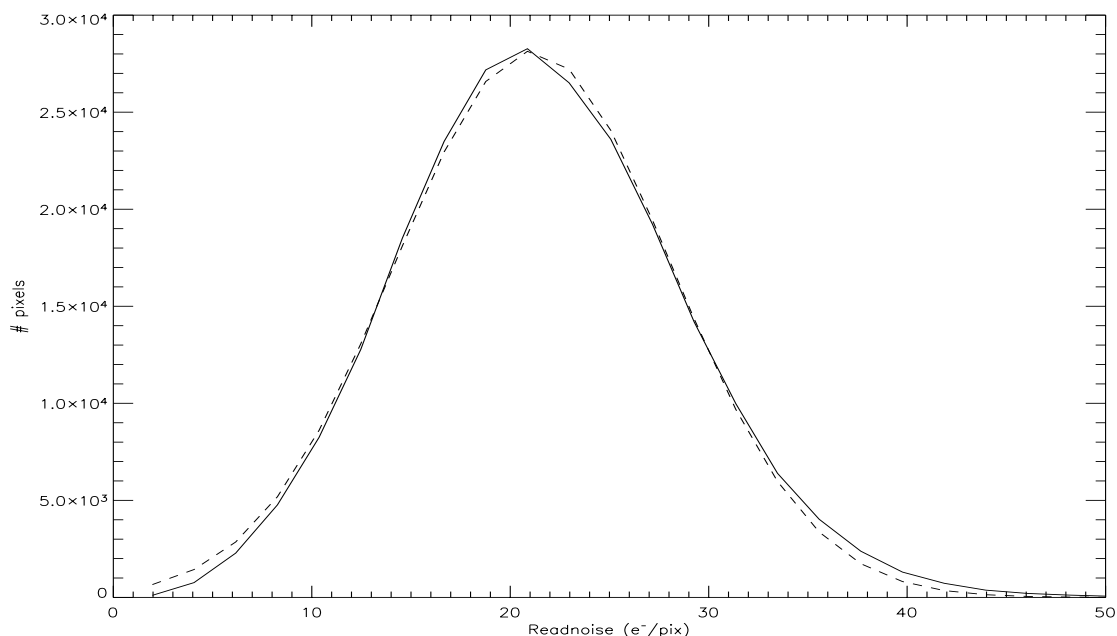


**Figure 1:** Typical histogram and best-fit Gaussian for a difference image of one quadrant of FPA64.

Method	Array Size (pixels)	Quadrant A (e <sup>-</sup> /pix)	Quadrant B (e <sup>-</sup> /pix)	Quadrant C (e <sup>-</sup> /pix)	Quadrant D (e <sup>-</sup> /pix)
Adjacent Differences	512	21.68 +/- 0.03	21.15 +/- 0.02	21.02 +/- 0.002	21.18 +/- 0.04
Line Fitting		21.43 +/- 0.06	20.75 +/- 0.01	20.49 +/- 0.09	20.79 +/- 0.05
Adjacent Differences	256	21.29 +/- 0.03	20.88 +/- 0.01	21.06 +/- 0.09	21.02 +/- 0.09
Line Fitting		21.01 +/- 0.001	20.11 +/- 0.28	20.36 +/- 0.22	20.40 +/- 0.14
Adjacent Differences	128	20.55 +/- 0.20	20.51 +/- 0.33	21.20 +/- 0.19	20.85 +/- 0.11
Line Fitting		20.95 +/- 0.77	20.26 +/- 0.18	20.65 +/- 0.32	20.05 +/- 0.54

**Table 4.** Median CDS readnoise values calculated from the IR05 STEP25 data. Subarray results are based on only 2 ramps per subarray size, resulting in low number statistics when calculating means and uncertainties (standard deviation).

## Recommendations

Due to the additional noise contribution from longer sample sequences, readnoise data should be taken with the RAPID sequence only.

## **Acknowledgements**

Many thanks to Sylvia Baggett, for helpful discussions on readnoise calculations.

## **References**

Hilbert, B. **Basic IDL Data Reduction Algorithm for WFC3 IR and UVIS Channel.** (WFC3 ISR 2004-10) <http://www.stsci.edu/hst/wfc3/documents/ISRs/WFC3-2004-10.pdf>. June, 2004.

Hilbert, B. **Results of WFC3 Thermal Vacuum Testing: IR Channel Dark Current.** (WFC3 ISR, in progress). 2005.

Malumuth, Eliot. **FPA64 Read Noise.** <http://dcl.gsfc.nasa.gov/private/wfc3/webwebdocs/fpa64/fpa64rn.pdf> 2004.